Shape transformation of Poly(butadiene)-b-poly(ethyleneoxide) plus DTAB compound micelles in aqueous solutions

Holger Egger, Anette Nordskog, Peter Lang*

Iwan-N.-Stranski-Institut for Physical and Theoretical Chemistry,

Technische Universität Berlin, Straße des 17. Juni 112, 10623 Berlin, Germany.

Astrid Brandt

Hahn-Meitner-Institut, Glienicker Straße 100, 14109 Berlin, Germany.

SUMMARY: The micellar shape of Poly(butadiene)-b-poly(ethyleneoxide) (PB-PEO) plus Dodecyltrimethylammoniumbromide (DTAB) compound micelles was investigated by light scattering, small-angle X-ray scattering and small-angle neutron scattering in dependence of the molar ratio between block copolymer and surfactant. The given block copolymer forms cylindrical micelles in binary aqueous solution, which transform to spherical aggregates upon the addition of a sufficiently high amount of DTAB. It is interesting to note that the micellar shape seems to be a bistable feature, in the sense that it depends not only on the molar ratio of BCP and DTAB but also in a predictable manner on the preparation procedure of the solution.

Introduction

Due to the mutual incompatibility of the molecular moieties, block copolymers (BCP) form micellar aggregates when dissolved in a solvent, which is selective for one of the two blocks. The structure of such aggregates has been subject of a large number of investigations[1)]. The majority of block copolymers exhibit a very high tendency to form spherical micelles in non-polar solvents. The density profiles of which can be adequately described by the spherical polymer brush model of Daoud and Cotton[2)]. In some reports anisometric micellar shapes have been studied, but such observations are limited to systems which are not in thermodynamic equilibrium[3,4)].

On the other hand a wide range of structural variety is observed in the field of low molecular weight surfactant solutions, ranging from spherical and cylindrical micelles over bicontinuous structures to inverted micelles[5)]. This variety can be qualitatively understood by geometric packing considerations[6)]. Accordingly, the micellar shape is determined by the relation

 CCC 1022-1360/00/$ 17.50+.50/0

between the effective area, *a,* of the surfactant's hydrophilic head group at the alkyl chain to water interface and the volume, *v*, of the hydrophobic chain. Large head group areas and small chain volumes favor the formation of spherical aggregates, while anisometric micelles will be formed if the packing parameter $P = v/al$ exceeds 1/3, where l is the effective length of the alkyl chain. At first glance it seems to be rather promising to adopt this concept to micelles formed by amphiphilic block copolymers in aqueous solution.

However, these simple packing considerations will obviously not hold for polymeric micelles, since for instance a polymer chain in a spherical brush may be markedly stretched from its unperturbed dimensions, i.e. reducing its lateral extension. Thus, it is not possible to change the packing parameter by simply varying the respective lengths, i.e. the degree of polymerization of the block copolymer. Further, the investigation of block copolymer micelles with a water soluble block is often hampered by the fact that the hydrophilic block is in the glassy state. Förster et al. have reported aggregates with various shapes in thermodynamic equilibrium from solutions of a block copolymer with a soft core block and a polyelectrolyte block as the hydrophilic moiety[7,8]. They show that the micellar shape of BCP can be tuned by the variation of the ionic strength, if electrostatic forces dominate the effective area of the hydrophilic block and the glass temperature of the block forming the micellar core is below the experimental temperature.

In the experiments reported in the present work, we have used a low molar mass cationic surfactant, dodecyltrimethylammoniumbromide (DTAB), to introduce charges to the core/water interface and thereby change the packing parameter of the Polybutadiene-*b*-Poly(ethyleneoxide) block copolymer aggregates.

Experimental Section

Sample. The blockcopolymer Polybutadiene-*b*-Poly(ethyleneoxide) (PB-*b*-PEO) with the block lengths 37 and 53 for the butadiene and the ethyleneoxide part, respectively, was synthesized by anionic polymerization according to the procedure described by Förster et al[9].

The cationic surfactant Dodecyltrimethyleammoniumbromide (DTAB) was purchased from Aldrich Chemicals and used without further purification, (Purity >97%).

For the light scattering experiments, high purity water from a Milli-Q water purification system by Millipore/Waters as the solvent was used. Whereas D_2O purchased from Sigma Fine Chemicals was used as solvent (Purity 99.8%) in the small-angle experiments (SANS and SAXS).

The individual solutions were prepared using two different successions of dilution steps, hereafter denoted as method A and method B:

Method A: A solution was prepared by weight, which contained the polymer PB-*b*-PEO and the surfactant DTAB at a given molecular ratio $r_m = n_{DTAB}/n_{BCP}$. The concentration of the surfactant was adjusted to a value far above the cmc of the surfactant in binary aqueous solution, which is 15mMol/l. The stock solution was diluted with water to maintain the molar ratio r_m constant while the surfactant was diluted to a concentration well below the cmc.

Method B: Separate solutions, the one containing only the surfactant at a concentration below the cmc, and the other containing the block copolymer, were mixed at volume fractions appropriate to obtain solutions of the same macroscopic compositions as the solutions prepared by method A.

The solutions for the light scattering measurements were filtered through filters with a pore size of 200 nm direct into dust free cylindrical quartz cells with an inner diameter of 0.8 cm. The solutions with a polymer weight fraction w_{BCP} of more than two percent and low values of r_m, prepared by method A and all solutions prepared by method B with $w_{BCP}>0.02$ could not be filtered without altering the concentration of the sample. The samples were subjected to the scattering experiment without filtration, which was justified by the finding that in none of these cases an influence of dust particles on the time auto correlation function of scattered intensity could be detected.

Light Scattering (LS). LS-measurements were performed with commercial equipment for simultaneous static and dynamic experiments from ALV-Laservertriebsgesellschaft (Langen, Germany). The light source used was the blue line (λ = 488 nm) of a Coherent 70/2 innova argon laser, operating at a power output of 100 mW. The primary beam intensity was monitored by means of a beam splitter and a four-segment photodiode, that was also used to control and adjust the primary beam position. Temperature control of the samples better than $\pm$ 0.1 K was achieved by a toluene thermostating bath, which also served as an index

matching bath. The detection unit was a photomultiplier run in a single-photon-counting mode attached to an ALV5000 correlator board with 256 multiple-τ channels and an initial lack time of 200 ns. Time autocorrelation functions were analyzed by fitting them with stretched exponentials to obtain mean relaxation times.

The static (integrated) intensity was normalized to the primary beam intensity and brought to absolute scale by using toluene as the reference for calibration.

Static as well as dynamic LS measurements were carried out in an angular range of $20°<\theta<150°$, that corresponds to a range the scattering vector $5.96 \cdot 10^4 < q < 3.32 \cdot 10^5\ cm^{-1}$ with $q = (4\pi/\lambda)n_0 \sin(\theta/2)$, where n_0 denotes the refractive index of the solvent. Both LS measurements were performed in steps of 5° and 30°, respectively.

Small-angle X-ray scattering (SAXS). The SAXS measurements were performed with a Kratky compact camera, equipped with a one-dimensional position sensitive detector, OED 50m, by MBraun (München, Germany). The active wire length was 50 mm, the sample to detector distance was 275 mm and angular calibration was achieved using a Ag-stearate powder sample. The X-ray tube was a conventional copper anode, operated at 30 mA and 30 kV. The primary beam was β-filtered with a nickel foil of 25 micrometers thickness located in front of the collimator and blocked with a 5 mm tungsten beam stopper in front of the detector. The intensity of the primary beam was measured with the movable slit method. A standard capillary for the Kratky camera by A. Paar was used as sample cell. All samples were measured over a time interval of 20 hours at 25±0.1°C. All scattering curves were normalized to the primary beam intensity and the scattering curve of the solvent was subtracted. The resulting excess scattering functions I(q) were desmeared and analyzed with Glatter's ITP package[10,11] which produces the corresponding pair-distance distribution function p(r) and the radially averaged electron density distribution ρ(r).

Small-angle neutron scattering (SANS). SANS measurements were performed at the light water cooled and moderated swimming pool type reactor of the Hahn-Meitner-Institut (HMI) Berlin, Germany, at instrument V4 which is located at the curved neutron guide NL 3A[12]. Neutrons were derived from a liquid hydrogen cold source and monochromated by a mechanical velocity selector. The mean de Broglie wavelength was set to $\lambda_0 = 0.60$ nm with a wavelength distribution with a fwhm of $\Delta\lambda/\lambda_0 = 0.1$. The two-dimensional ^{3}He detector with

64 x 64 elements of 10 x 10mm^2 was positioned at sample-to-detector distances of 1, 4 and 16 m to cover a range of momentum transfer of 0.03 nm^{-1} < q < 3.6 nm^{-1} after radial averaging. Quartz cells with a path length of 1 mm were used as sample containers which were inserted into aluminium sample holders. All the measurements were performed at a temperature of 25°C.

According to HMI standard procedure, the primary data were reduced and evaluated in two steps. In the first step, sample cell scattering and background scattering were subtracted from the raw data. The resulting two-dimensional array was normalized to the scattering of H_2O and subsequently radially averaged. In the second step the solvent scattering function was subtracted and the obtained one-dimensional scattering functions were analyzed with Glatter's software as described for the SAXS measurements.

Atomic Force Microscopy (AFM). A binary solution containing 20 mg/ml of the BCP was spread onto a hydrophilized Si-wafer, freeze dried and subsequently investigated by AFM with an Atomic Force Microscope Multimode Nanoscope 3 from Digital Instruments. The measurements were carried out at 25 °C using the tapping mode. For the investigations the top layer of the sample was removed to obtain images from the interior of the sample.

Results and Discussion

Binary aqueous solutions of the block copolymer Polybutadiene-b-Poly(ethyleneoxide) (PB_{37} – PEO_{53}) are turbid and birefringent at polymer mass fractions above $w_{BCP} = 0.02$.

In Fig.1 we show an Atomic Force Microscopy (AFM) image obtained from a solution of pure polymer in water at a concentration of 20 mg/ml, that had been spread onto a Si-wafer and subsequently freeze dried. The picture shows a network of long cylindrical aggregates with a cross-sectional diameter of around 30 nm, the length of which cannot be determined.

Upon addition of the ionic surfactant dodecyltrimethylammoniumbromide (DTAB) to the turbid binary mixtures, they transform to clear and optically isotropic solutions. Assuming that the low mass surfactant forms compound micelles with the blockcopolymer this transformation may be understood in terms of the concept of packing parameters and natural leads to a growing mean effective lateral area per headgroup by virtue of the long ranging electrostatic repulsion. On the other hand, the chain volume in the hydrophobic core is not significantly effected by the introduction of low molar mass molecules, and consequently the

packing parameter of the interface will decrease, which would favor the formation of spherical micelles. In what follows we will discuss experimental evidence, which show this line of thought to be correct.

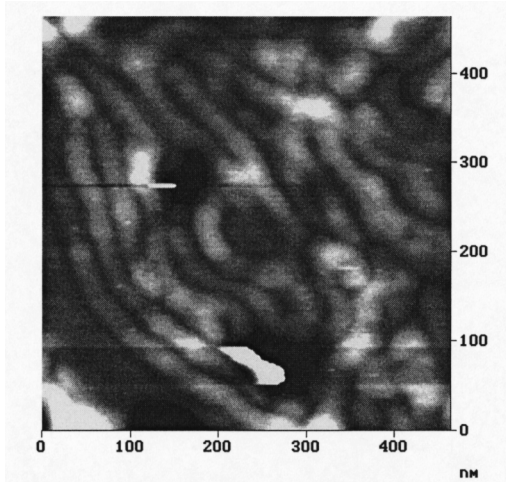

Fig.1: AFM-Image of pure BCP. For details of the sample preparation see text. The cylindrical aggregates have a cross-sectional diameter of about 30 nm.

Light scattering: We performed measurements of three different sample series prepared by method A: (i) A dilution series of binary mixtures of the BCP in water, (ii) a series with varying polymer concentration and constant molar ratio $r_m = n_{DTAB}/n_{BCP}$, namely r_m=42 (far above the point of optical clearing) and (iii) a series of samples with constant polymer concentration (20 mg/ml) and varying r_m in the range $0<r_m<7$ which covers the range of r_m where the optical clarification occurs.

The results of the static light scattering experiments from first series and the second series are displayed as Zimm-plots in Fig.2 and 3 respectively.

According to Zimm[13], the mass average molar mass M_w and the radius of gyration R_g of the scatterers can be determined from a linear extrapolation of the inverse product of particle scattering factor and molar mass $(P(q)M_w)^{-1} = \lim_{c\to 0} \frac{Kc}{R(q)}$ versus the square of the scattering vector. As can be seen from Fig.2, in this case it is not possible to perform an extrapolation of the scattering data to zero scattering vector in a reliable manner. Thus it is not possible to determine the molar mass M_w and the radius of gyration R_g of the aggregates. For the latter an estimate for the minimum value can be given, i.e. $R_g \geq 300$ nm.

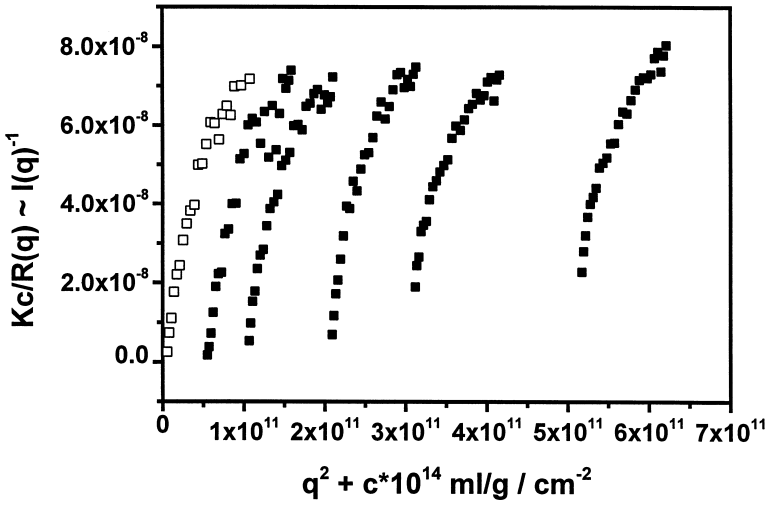

Fig.2: Zimm plot of the static scattering from a dilution series of pure BCP in water. The concentrations range from 0.45 – 1.33 mg/ml. Open symbols represent extrapolated data for c = 0, i.e. the inverse product of particle scattering factor multiplied by the particle molar mass $(M_wP(q))^{-1}$.

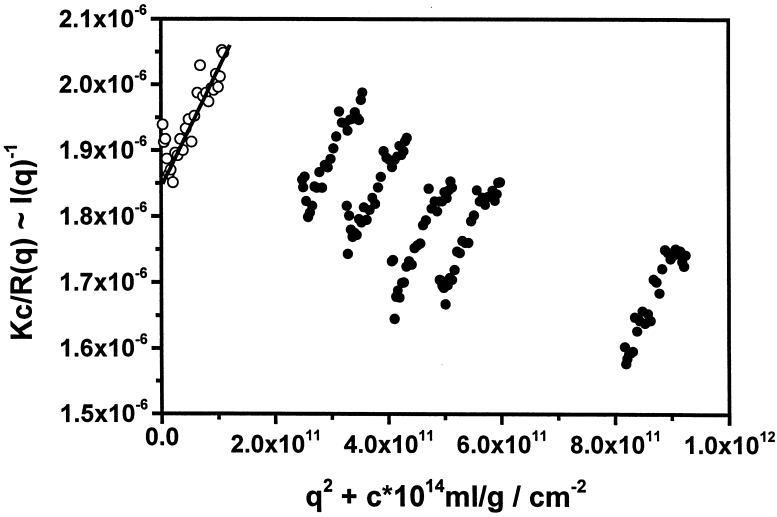

Fig.3: Zimm plot of the static scattering from a dilution series of BCP and DTAB in water with a constant $r_m = 42$ and the overall concentrations of the dispersed material ranging from 2.45 – 8.14 mg(BCP + DTAB)/ml. Open symbols represent extrapolated data for c = 0, i.e. the inverse product of particle scattering factor multiplied by the particle molar mass $(M_wP(q))^{-1}$.

On the other hand, in dynamic scattering experiments we always found the relaxation constants to be strictly proportional to the square of the scattering vector $\Gamma = \langle \tau \rangle^{-1} \propto q^2$ with $<\tau>$ being the mean relaxation time of the time autocorrelation function of the scattered intensity. Consequently it was possible to determine the z-average diffusion coefficient D_z of the system reliably by an extrapolation procedure similar to that applied in a Zimm-plot. This value was used to calculate the hydrodynamic R_h=75 nm radius according to the Stokes Einstein equation.

Differently from the findings in the first series it was possible to extrapolate the static light scattering data from the second series in a Zimm-plot (cf. Fig.3). This procedure yields a radius of gyration R_g= 17 nm and a mass average molar particle mass of $M_w=5.4 \cdot 10^5$ g/mol. It has to be emphasized that the value of R_g is at the lower limit of resolution in light scattering and therefore bears a comparatively large uncertainty. The negative slightly bent concentration dependence of the inverse scattered intensity, which corresponds to a negative second osmotic virial coefficient, hints at attractive interaction forces between the micelles being present. This is very surprising at first glance, since the compound micelles are charged and one would interaction forces expect to be repulsive. However, one might speculate that we are dealing with an effect similar to that observed in low ionic strength polyelectrolyte solutions[14]. Indeed there is a number of publications[15-18] which suggest that there is a region of attractive potential generated by purely electrostatic interactions, leading to the formation of domains, the size of which is independent of concentration [14].

The dynamic light scattering measurements on this series yield a hydrodynamic radius of R_h=15 nm. For comparison, the apparent hydrodynamic radius measured in a binary solution of DTAB in water is about 1.2 nm. It is thus quite safe to assume that we do not observe DTAB micelles in the case discussed and from the fact that the autocorrelation functions are very close to single exponential it is obvious that we neither observe mixtures of DTAB micelles and BCP micelles. We are therefore quite sure that DTAB and the blockcopolymer form compound micelles.

According to Burchard et al[19] the ratio of the radius of gyration to the hydrodynamic radius $\rho = R_g / R_h$ is sensitive to the shape of the scatterers. While spherical particles have ρ-values of 0.77, cylindrical objects have values of ρ>2 depending on their aspect ratio. In the present case the micellar aggregates have values of ρ>4 in the absence of low molar mass surfactant, while it drops to about ρ≈1, if a sufficient amount of DTAB is present. This is clear evidence

for a shape transformation of the aggregates from cylindrical to close to spherical, which is induced by the presence of charged groups at the hydrophobic core-water interface in the compound micelles.

For the third sample series, containing a constant polymer concentration of 20.6 mg/ml and a molar ratio of DTAB and blockcopolymer varying from r_m=0 to r_m=7, we performed only dynamic light scattering measurements and calculated apparent hydrodynamic radii $R_{h,app}$. In Fig.4, $R_{h,app}$ is plotted as a function of the molar ratio r_m. At ratios $r_m \leq 2$ the apparent hydrodynamic radius has values of about 100 nm. At molar ratio r_m 2-4 we observe a steep decrease of $R_{h,app}$ from 100 nm to around 17 nm, but further increasing molar ratios do not effect $R_{h,app}$ anymore.

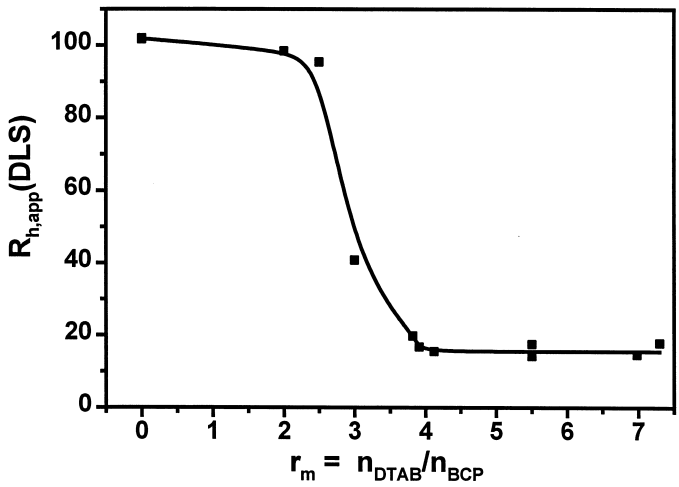

Fig.4: Apparent hydrodynamic radii resulting from the dynamic light scattering measurements plotted versus r_m for solutions of BCP plus DTAB in water containing a constant concentration of BCP, c_{BCP} = 20 mg/ml.

Small-angle X-Ray Scattering (SAXS) experiments were carried out for solutions with a block copolymer mass fraction w_{BCP} = 0.02 and different amounts of surfactant varying the molar ratio r_m from 0 to 14. For all values of r_m the excess scattering curves look qualitatively the same. Due to the poor scattering contrast all curve become extremely noisy at comparatively low scattering vectors, e. g. $q>1$ nm^{-1}. They show a local minimum of the scattered intensity at about $q \approx 0.6$ nm^{-1}, the exact position of which is correlated with the molar

ratio r_m. The scattering curves from the samples with r_m=1 and 14 are shown as representative examples in Fig.5.

The overall shape of the resulting pair distance distribution functions p(r) is generally same for all samples, which is puzzling at first glance, since one would expect the p(r)-function of a cylindrical particle to be clearly distinguishable from that of a sphere. However, if the length of the long axis of the cylindrical particle is far off the range covered by the scattering vector in the SAXS-experiment, it will be sensitive only to the cross sectional pair distribution function. Consequently a spherical and a cylindrical particle with large aspect ratio will show almost the same scattering function and p(r)-function, if the radius of the sphere and the cross sectional radius of the cylinder are equivalent. This fact is illustrated by means of model calculations in Fig.6, where we compare the particle scattering factors and the p(r)-functions of a compact sphere with a diameter of 30 nm and a compact cylinder, which is

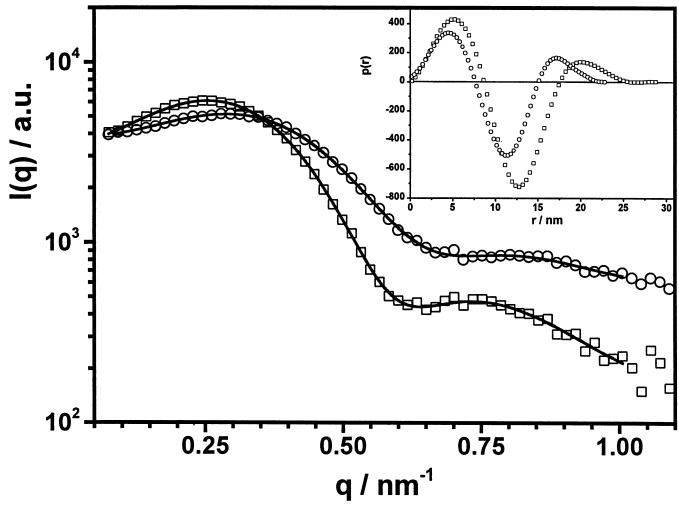

Fig.5: SAXS curves from solutions with constant BCP-weight fraction, w_{BCP} = 0.02 and different molar ratio r_m. Open symbols are desmeared experimental data (□) : r_m = 1 and (○) : r_m = 14 and full lines are best fits, the resulting pair distance distribution functions depicted in the inset.

300 nm in length and has a cross sectional diameter of 30 nm[20]. In our experiment the maximum dimension D_{max} of the particles, i. e. the value of r at which the pair distance distribution function decays to zero, apparently depends to a certain extend on the molar ratio

r_m. With increasing r_m D_{max} decreases slightly starting at a value of around 29 nm for the pure polymer aggregates down to 24 nm for the highest DTAB concentration. This might be misinterpreted in the sense that the cross-sectional diameter of the cylindrical micelles is larger than the diameter of the spherical aggregates. However, as can be seen from Fig.6 the maximum dimension in the p(r)-function of the cylinder exceeds the cross sectional diameter significantly, while for the spherical particle the maximum dimension coincides with the twofold of the sphere radius.

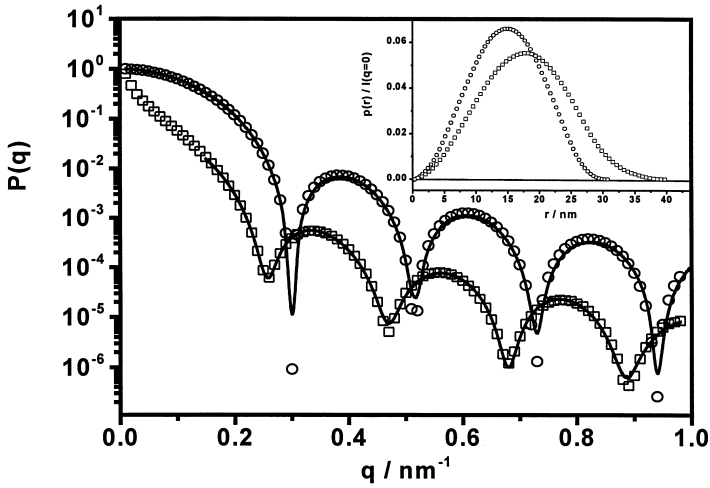

Fig.6: Particle scattering factors P(q) from model calculations for spheres (○) and cylinders (□) with a diameter and a cross-section of 30 nm respectively. The inset shows the corresponding p(r) functions.

Accordingly, we can determine the radius of the spherical micelles at r_m>4 by $D_{max}/2$=12 nm. This result is in fair agreement with the value of the hydrodynamic radius R_h=15nm as determined by dynamic light scattering. Taking $D_{max}/2$ as the value for the geometrical radius of the micelle the resulting value of ρ=0.71 is actually very close to the theoretical value for a hard sphere.

The fact that the pair distance distribution functions exhibit parts with negative sign reflects the inhomogeneous electron density profile of the particles in all cases. The excess electron density functions $\Delta\rho(r)$, which can be calculated from the p(r)-functions by numerical deconvolution give a more detailed picture of the structure of the micelles. The cores of the aggregates consist of polybutadiene which has a significantly lower electron density than the

solvent, which one would expect concerning the bulk values of the mass density of both compounds. On the contrary, polyethyleneoxide in the shell of the micelle has a slightly higher electron density than water, which was also found for the hydrophilic part of micelles, that consist of low molar mass oligo(ethyleneoxide)-n-alkylether surfactants. This shows that the blocks of the BCP are arranged in the same manner in the cylindrical as in the spherical micelles, and that the only difference of the two structures is the extension in the one dimension.

To further confirm the structural details of the blockcopolymer micelles we performed **Small-angle Neutron Scattering (SANS)** experiments, which cover a larger q-range than accessible in SAXS, especially at low q values, from where one would expect to gain information about the length of cylindrical particles. The SANS experiments were carried out with the same samples as the SAXS-measurements.

Qualitatively the SANS curves support the picture of a shape transformation of the micelles in dependence on the molar ratio, which we had deduced from light scattering and SAXS measurements. This is most clearly envisioned in a double logarithmic plot of the scattering curves as shown in Fig.7. In this representation we observe a region of zero slope at small q-values for the samples with $r_m \geq 4$. For smaller values of r_m the slope at small scattering vectors becomes finite and increases continuously with decreasing r_m. In parallel the scattering intensity at higher q-values increases, which is in line with the picture of a structural change from cylindrical to spherical micelles with increasing molar ratio of surfactant and blockcopolymer.

However, it has to be noted that the cylindrical length can not be determined from the present SANS-data reliably, which is obvious from the non-zero slope in the double logarithmic representation of the scattered intensity.

In the inset of Fig.7 we have depicted the pair distance distribution functions extracted from the corresponding SANS-curves. Since we could not obtain the full information on the length of the cylindrical particles we omitted the points with $q<0.25nm^{-1}$ in the calculation of the p(r)-function in this case. Consequently the curves shown, represent the cross sectional p(r)-function for the cylindrical micelles as in the case of the SAXS-experiments, and as to be expected the p(r)-curves from the spherical particles and the cylinders appear to be very similar. Differently from the SAXS experiments these p(r)-functions do not have parts with negative sign, which reflects the fact that the polybutadiene block as well as the poly(ethylenoxide) block have a lower scattering length density than D_2O.

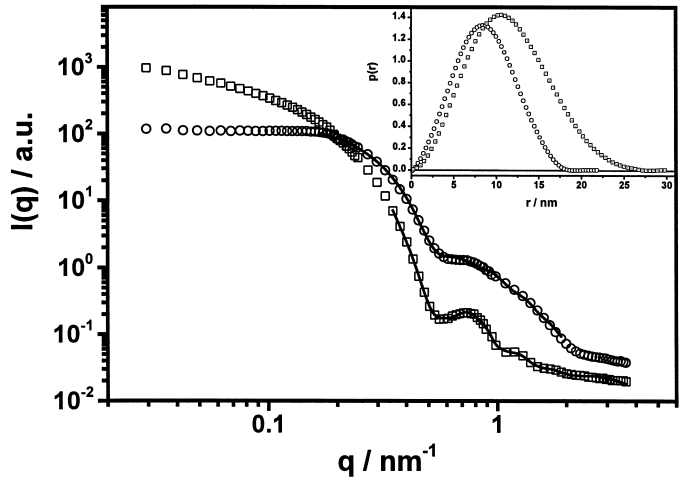

Fig.7: Scattering curves from the SANS-measurements of solutions of constant BCP-concentration, w_{BCP} = 0.02 and different molar ratios of surfactant and blockcopolymer (□): r_m = 1, (○): r_m = 14. The inset shows the corresponding pair distance distribution functions calculated by ITP.

Dependency on method of preparation. As already mentioned the measurements described so far were performed with solutions prepared by method A. If we apply method B to prepare solutions with same macroscopic composition, the above described transformation does not take place. Fig.8 shows the time autocorrelation functions from dynamic light scattering recorded at a scattering angle of Θ=90° of two solutions both containing a polymer concentration of 0.5 mg/ml and a molar ratio r_m = 42 (this corresponds to a DTAB concentration of 4.8 mMol/L which is about a third of the cmc of DTAB in water), one of which was prepared using method A and the other using method B. The time of relaxation for the sample prepared by method B is about one order of magnitude higher than for sample prepared by method A. This corresponds to a difference in the apparent hydrodynamic radius of $R_{h,app}$=15 nm for method A and 71 nm for method B.

To our knowledge, this or a similar kind of different behavior of two solutions, which have the same macroscopic composition, was not reported in literature before and we can only speculate about the physical reason. Very likely it is due to the respective dilution procedure of the solutions With method A the surfactant is present in the stock solution at a

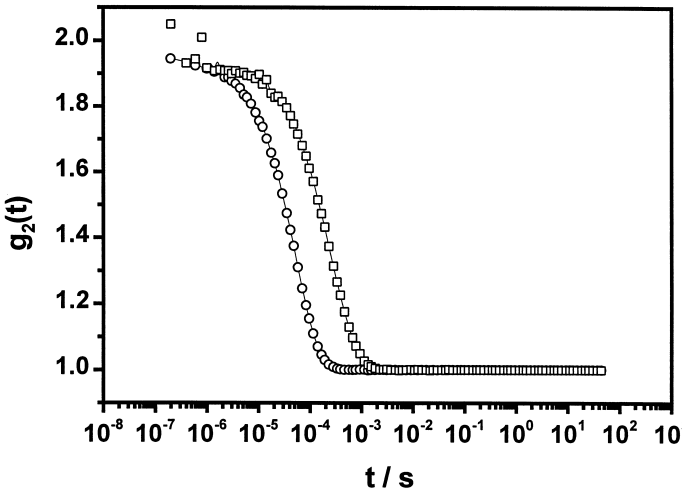

Fig.8: Time autocorrelation functions of the scattered intensity $g_2(t)$ from dynamic light scattering measurement of two solutions of the same macroscopic composition. Both solutions have a polymer concentration of 0.5 mg/ml and a molar ratio of DTAB to BCP r_m = 42 prepared by method A (○) and method B(□), respectively.

concentration above the cmc of the surfactant. Accordingly the chemical potential of the surfactant is high enough to cause surfactant aggregation. In the present case this leads to the formation of compound micelles with the blockcopolymer and consequently to the transformation from wormlike blockcopolymer micelles to spherical mixed micelles in the stock solution. Apparently, the following dilution does not effect the micellar shape, although the overall surfactant concentration becomes smaller than the critical value for micelle formation.. On the other hand, using method B, the concentration of DTAB in the polymer solution is below the cmc of the surfactant at any time. Consequently, the chemical potential is never sufficiently high to drive the DTAB molecules to adsorb at the interface between the butadiene core and the aqueous part of the blockcopolymer micelles. Therefore the blockcopolymer micelles in solutions prepared with method B retain their original shape. The proposed mechanism requires that the amount of molecularly dispersed DTAB depends on the method of preparation, which can be verified by conductivity measurements. This is subject of ongoing work and will be discussed in a forthcoming publication.

Since samples prepared by method A as well as by method B may have the same macroscopic composition, but contain different kinds of aggregates, only one of these samples can be in thermodynamical equilibrium. Although the DTAB concentration was twice the cmc

originally in the stock solution prepared by method A, it drops to one third of the cmc upon dilution. This implies that the DTAB molecules should dissolve molecularly dispersed in the solvent, while the BCP micelles maintain the shape which was originally induced by the surfactant. One might also speculate that the separation of the compound micelles into pure BCP-micelles and DTAB unimers is kinetically hindered. Both scenarios would mean that the spherical micelles induced by the preparation using method A represent a metastable state, while method B produces micelles in the thermodynamical stable state. However, the scattering behavior of a solution prepared by method A, does not change over a period of time of at least a few months, and therefore it is impossible to judge unambiguously from our experimental data which state is the stable one.

Conclusion

Combining the results from a variety of scattering experiments, we conclude that large cylindrical aggregates of PB-*b*-PEO in water, transform into small spherical mixed micelles upon the addition of the cationic surfactant DTAB. This transformation can be qualitatively explained by the following argument. In the binary mixture the BCP molecules are assembled in large cylindrical aggregates. If the amount of DTAB, which is added to such a solution, is above the cmc, mixed micelles are formed. The driving force for the formation of compound micelles, instead of two separate species of aggregates, is probably due to the dilution of charges by embedding the cationic surfactant headgroup in the matrix of electrically neutral ethyleneoxide segments. On the other hand, the effective area of the cationic headgroups is very large due to the long ranging Coulomb interaction, while the volume of the hydrophobic micellar core is only little effected by the introduction of the surfactants dodecyl chain. Consequently the natural curvature of the internal interface will increase upon the adsorption of DTAB molecules to it, which eventually leads to the observed shape transformation of the micelles.

Acknowledgment. We thank E. Krämer (MPI für Kolloid- und Grenzflächenforschung, Golm, Germany), for the gift of the PB-b-PEO sample and U. Mähr and T. Fütterer for their help with the AFM experiment. Financial support by the Deutsche Forschungsgemeinschaft (Sonderforschungsbereich 448) is gratefully acknowledged.

References

1. S. Förster, M. Zisenis, E. Wenz, M. Antonietti, *J. Chem. Phys.* **104**, 9959 (1996) and references therein.
2. M. Daoud, J. P. Cotton, *J. Phys. (Paris)* **43,** 531 (1982).
3. J. P. Spatz, A. Röscher, M. Möller, *Adv. Mater.* **8,** 795 (1996).
4. N. S. Cameron, M. Corbierre, A. Eisenberg, *Can. J. Chem.* **77,** 1 (1999) and references therein.
5. For an overview see for instance *Micelles, Membranes Microemulsions and Monolayers*, W. Gelbart, A. Ben-Shaul und D. Roux (Eds.), Springer, New York, 1994.
6. J. Israelachvili *Intramolecular & Surface Forces* Academic Press, London, 1992.
7. S. Förster, N. Hermsdorf, W. Leube, H. Schnablegger, M. Regenbrecht, S. Akari, P. Lindner, C. Böttcher, *J. Phys. Chem. B* **103,** 6657 (1999).
8. M. Regenbrecht, S. Akari, S. Förster, H. Möhwald, *J. Phys. Chem. B* **103,** 6669 (1999).
9. S. Förster, E. Krämer, *Macromolecules* **32**, 2783 (1999).
10. O. Glatter, *Acta Phys. Austriaca* **47**, 83 (1977).
11. O. Glatter, *J. Appl. Cryst.* **14**, 101 (1981).
12. U. Keiderling, A. Wiedenmann, *Physica B* **213&214**, 895 (1995).
13. B. H. Zimm, *J. Chem. Phys.* **16**, 1099 (1948).
14. B. D. Ermi, E. J. Amis, *Macromolecules* **31**, 7378 (1998).
15. J. Ray, G. S. Manning, *Langmuir* **10**, 2450 (1994).
16. N. Grønbech-Jensen, R. J. Mashl, R. F. Bruinsma, W. M. Gelbart, *Phys. Rev. Lett.* **78**, 2477 (1997).
17. B. Y. Ha, A. Liu, *Phys. Rev. Lett.* **79**, 1289 (1997).
18. K. S. Schmitz, *Langmuir* **13**, 5849 (1997).
19. W. Burchard, M. Schmidt, W. H. Stockmayer, *Macromolecules* **13**, 580 (1980).
20. P. Mittelbach, G. Porod, *Acta Phys. Austriaca* **14**, 405 (1961).